ARTICLE NO. 78-981R

Oxidizer Size Distribution Effects on Propellant Combustion

J.P. Renie,* J.A. Condon,† and J.R. Osborn‡
Purdue University, West Lafayette, Ind.

The effect of the oxidizer size and size distribution on the pressure and temperature sensitivity for a nonaluminized composite solid propellant was investigated using a new mathematical model called the Petite Ensemble Model. Calculations were made using the new model, taking into account the oxidizer size and size distribution in determining the burning rates, rate exponents, and temperature sensitivities. Results were obtained for both unimodal and bimodal propellants with oxidizer particle sizes ranging from ultrafine (0.7 μ) to coarse (400 μ). For unimodal propellants, it was determined that the burning rate was higher for the smaller oxidizer sizes, as would be expected. Moreover, the rate exponent was larger for the small and large oxidizer particles with a minimum exponent obtained for some intermediate oxidizer diameter. Temperature sensitivity was found to be higher for propellants with larger oxidizer particles. However, it was found that the temperature sensitivity was constant for small particles. It was shown that for large particles, the temperature sensitivity and rate exponent decreased as the oxidizer distribution was widened.

Nomenclature

c = constant in St. Robert's burning rate law, Eq. (3)
D = oxidizer diameter
F = oxidizer mass distribution function
n = pressure exponent in St. Robert's burning rate law, Eq. (3)
p = pressure
r = burning rate
T_0 = initial solid propellant temperature
α = oxidizer mass fraction
π_K = temperature sensitivity, Eq. (5)
σ = oxidizer mode width parameter
σ_p = temperature sensitivity, Eq. (4)

Superscript

$\bar{(\ )}$ = mean value

Subscripts

$(\ )_d$ = monodisperse pseudopropellant
$(\ )_{ox}$ = oxidizer

I. Introduction

THE combustion characteristics consisting of burning rate, pressure exponent, and temperature sensitivity for a composite solid propellant are highly dependent upon the physical nature of the oxidizer; that is, the size and size distribution of each of the individual oxidizer modes. Earlier steady-state solid propellant combustion models for composite propellants considered the particle sizes of the oxidizer to be represented by a single characteristic oxidizer particle size. The Petite Ensemble Model (PEM) described below treats the oxidizer in a more realistic fashion in that both the size and size distribution of the individual oxidizer modes comprising a composite solid propellant are considered. The PEM is capable of considering any number of oxidizer modes each having a different size distribution.

Calculations are presented which describe that model's capability for predicting the effect of the oxidizer size and size distribution of the combustion characteristics of a composite solid propellant.

Received July 18, 1978; presented as Paper 78-981 at the AIAA/SAE 14th Joint Propulsion Conference, Las Vegas, Nev., July 25-27, 1978; revision received Feb. 15, 1979. Copyright © American Institute of Aeronautics and Astronautics, Inc., 1978. All rights reserved. Reprints of this article may be ordered from AIAA Special Publications, 1290 Avenue of the Americas, New York, N.Y. 10019. Order by Article No. at top of page. Member price $2.00 each, nonmember, $3.00 each. **Remittance must accompany order.**

Index categories: Combustion Stability, Ignition and Detonation; Combustion and Combustor Designs.

*Student, School of Mechanical Engineering. Student Member AIAA.

†Student, School of Mechanical Engineering. Presently, Hercules Powder Company, Cumberland, Md. Student Member AIAA.

‡Professor, School of Mechanical Engineering. Associate Fellow AIAA.

II. The Model

The PEM is a steady-state combustion model which combines a statistical formalism[1] and a combustion model similar in several respects to the Beckstead, Derr, and Price (BDP) model.[2] The addition of the statistical formalism permits a description of the oxidizer particle size and size distribution which makes the model more realistic in terms of actual propellant formulations.

Oxidizer Size and Size Distribution

Since the PEM is capable of describing the combustion of a solid propellant having a distribution of oxidizer sizes, it is useful to define two independent parameters that describe a particular oxidizer distribution. They are the mean diameter $\bar{D}$ and the mode width parameter σ. Then the mass distribution of a typical oxidizer grind can be characterized by a log normal distribution function, $F_{ox,d}$. Thus,

$$F_{ox,d} = \frac{1}{(2\pi \ell n\sigma)^{1/2}} \exp\left[-\frac{1}{2}\left[\frac{\ell nD - \ell n\bar{D}}{\ell n\sigma}\right]^2\right] \qquad (1)$$

The mean diameter $\bar{D}$ is termed the 50% weight mean diameter, since half of the oxidizer's mass is composed of particles of diameter less than $\bar{D}$. The term σ represents the actual width of the distribution about the mean oxidizer particle diameter, $\bar{D}$. Integration of this expression from one particular value of oxidizer particle diameter to another results in the mass fraction of oxidizer within that specified mode having diameters within those integration limits.

A mode width parameter σ equal to unity corresponds to a monodisperse oxidizer mode; that is, all oxidizer particles in the mode are of one diameter, $\bar{D}$. A mode width parameter exceeding unity represents a polydisperse oxidizer mode distribution. In a polydisperse mode, the oxidizer mass is distributed about the 50% weight mean diameter; the larger the value of σ, the wider this distribution of oxidizer mass about $\bar{D}$.

To illustrate the accuracy of the assumption that actual oxidizer grinds fit log normal distributions, log probability

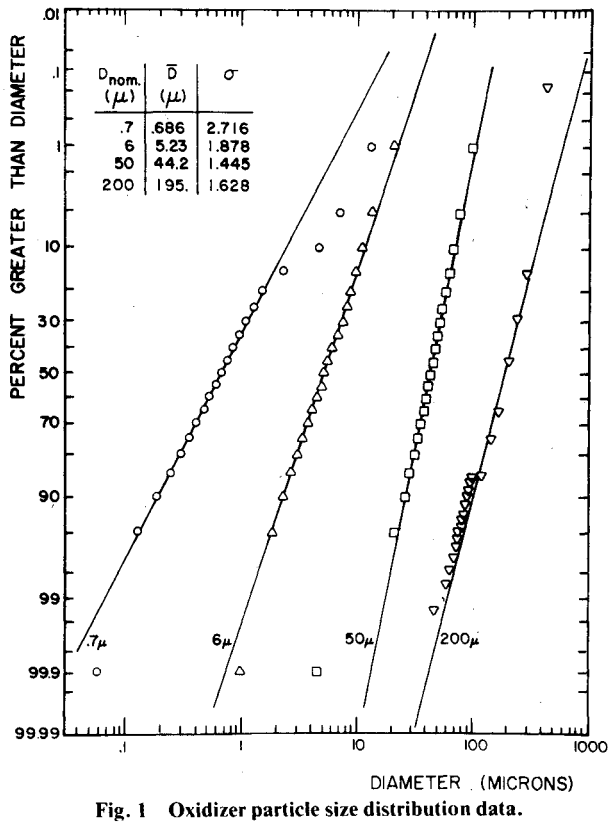

Fig. 1 Oxidizer particle size distribution data.

plots of oxidizer weight percent greater than diameter vs particle diameter are presented in Fig. 1 for four different experimental AP oxidizer grinds.[5]

Since a straight line on this type of graph represents a true log normal distribution, a linear least-square fit of each set of data was obtained, and the mean diameter $\bar{D}$ and mode width parameter σ for each fit of the grind data are presented on the figure. A vertical line on this figure would indicate the monodisperse ($\sigma = 1.0$) case, and the more polydisperse a distribution becomes, the less the slope of this line. Mode width parameters for typical AP oxidizer grinds run from near monodisperse to very polydisperse (a σ of the order of 3.0). This log normal polydispersion of oxidizer particle size was exhibited by all eight oxidizer grinds of Ref. 5, although only four are shown.

By utilizing the log normal distribution function, each oxidizer mode within a composite propellant can be represented by two independent parameters, the 50% weight mean diameter $\bar{D}$ and the mode width parameter σ. In addition to these two parameters, each oxidizer mode is characterized by a given oxidizer mass fraction, such that the summation of the mass fractions of all the modes equal the total oxidizer mass fraction for the composite propellant considered. The overall propellant oxidizer distribution function F_d utilized in the burning rate expression given in the next section, is the summation of the oxidizer mass distribution function of each mode, each being multiplied by their respective value of oxidizer mass fraction. With this more realistic description of the oxidizer incorporated within the PEM, the effect of the size and size distribution of the oxidizer mass on burning rate, pressure exponent, and temperature sensitivity can be determined.

Burning Rate

To determine the burning rate of a polydisperse propellant, the propellant is first mathematically rearranged into a series of monodisperse pseudopropellants. The mass flux from the entire polydisperse propellant surface and, consequently, its burning rate can then be determined by a statistical summation process of all the mass fluxes from these monodisperse pseudopropellants. The monodisperse mass fluxes are determined from the unit flame combustion model which mathematically describes the combustion of a single perchlorate particle submerged in an annulus of fuel. For that particle, the burning rate is obtained from a solution to a set of simultaneous equations which include the surface geometry and surface temperature. Imbedded in those equations are the geometrical and combustion variables describing the propellant in detail. A more complete description of the combustion model is given in Ref. 4.

Utilizing this statistical methodology, a mathematical expression for the total propellant burning rate, $\bar{r}$,[3,4] can be written in the following form:

$$\bar{r} = \int_D \frac{r_d}{\alpha_d} F_d \, d\ell n D \tag{2}$$

In this expression, r_d, α_d, and F_d are the burning rate, oxidizer mass fraction, and oxidizer distribution function, respectively, for each monodisperse pseudopropellant of a given oxidizer diameter (as designated by the subscript, d). The monodisperse burning rates, r_d, are calculated from the monodisperse mass fluxes.

In this manner, the total propellant burning rate is expressed in terms of propellant formulation variables and the monodisperse pseudopropellant burning rates. The propellant formulation variables are selected in the form of the oxidizer particle size and size distribution, the oxidizer mass fraction, and the other oxidizer/binder characteristics. The integration over all oxidizer particles sizes for the burning rate for a polydisperse propellant forms the Petite Ensemble Model.

The PEM just described thus permits consideration of a real propellant having an oxidizer particle size distribution. This model represents a significant improvement over the more conventional models,[2,6,7] which require that a single particle size be selected to represent the polydispersion of oxidizer particle sizes present in all real propellants.

Pressure Exponent

In order to determine the pressure exponent n in the St. Robert's law

$$\bar{r} = cp^n \tag{3}$$

the burning rate is determined using the PEM for three different values of pressure—3.45, 6.89, and 13.79 MPa, and for a constant value of initial temperature, 294 K. Then, a linear least-square fit of the calculated points on a logarithmic rate vs pressure plot is determined. The reported value of the pressure exponent at a pressure of 6.89 MPa is the slope of this "fitted" line. This technique for determining the pressure exponent is similar to that of the experimental study[5] used for comparison purposes.

Temperature Sensitivity

A number of related parameters may be defined for describing the temperature sensitivity characteristics of a solid propellant. Since the PEM is concerned with the determination of the burning rate, the effect of the initial propellant temperature T_0 on the burning rate is one of the parameters for which computations have been made. Thus,

$$\sigma_p = \left.\frac{\partial \ell n \bar{r}}{\partial T_0}\right|_{p=\text{const}} \tag{4}$$

Another parameter of interest is the temperature sensitivity π_K, which is related to σ_p and the pressure exponent n. Thus,

$$\pi_K = \sigma_p / (1 - n) \tag{5}$$

Therefore, the calculated values of both σ_p and π_K are presented.

In order to calculate σ_p, the burning rate is determined for initial solid propellant temperatures of 284, 294, and 304 K. A second-order fit of these points on a semilogarithmic burning rate vs initial temperature plot yields σ_p, which is the slope of this fit at an initial temperature of 294 K.

III. Determination of Propellant Constants

As is the case with other steady-state burning rate models, the PEM requires the use of several constants, such as the activation energies and the pre-exponential frequency factors for the several reactions, the heats of the fuel pyrolysis and the oxidizer decomposition, and the specific heats and thermal conductivities for both the gas and the solid phases. Some of these input parameters are known only to a small degree of precision. In order to determine the appropriate values for these constants, experimental burning rate data were used.[5]

The burning rate and pressure exponent were determined experimentally for a series of AP/HTPB nonmetallized propellants[5] at a pressure of 6.89 MPa and an initial temperature of 294 K. These composite propellants were formulated from eight individual oxidizer grinds with the total oxidizer mass fraction held constant at 87.4% for each blend.

The theoretical burning rates and pressure exponents were obtained using the PEM and subsequently compared to the experimental values. In this manner the numerical value for the input constants were varied, each within certain prescribed limits, until the best fit of the experimental data, both burning rate and pressure exponent, was obtained.

Table 1 gives the values for some of the more important input parameters, along with some of the better known constants such as the fuel and oxidizer solid phase densities. Once the values for these parameters had been established, they were not changed during the calculations for burning rate, burning rate exponent, and temperature sensitivity.

Figures 2 and 3 present the results for the experimental data. Figure 2 depicts the predicted burning rate vs the experimental rate for the twenty-one propellant configurations considered, and Fig. 3 presents the PEM prediction of pressure exponent vs the experimental exponent for the same propellants. The small numbers beside the data points in Figs. 2 and 3 refer to the ith propellant of Ref. 5's series SD-III-88-i. These propellants are primarily trimodal, so in that case there are three separate values for $\bar{D}$ and σ characterizing a propellant. In both cases, the PEM prediction matched the experimental data quite well with over 70% of the data within the 10% band. In some instances for which the experimental value was outside or near the 10% theoretical bands, it was noted that the modal structure of the oxidizer was comprised of very large and very small particles. In such cases, the assumption of noninteracting unit flames may be a poor one.[8]

Table 1 PEM input parameters

Heat of pyrolysis of fuel	1812 kJ/kg
Density of fuel	903 kg/m^3
Pre-exponential for fuel surface decomposition	40,000 kg/m^2·s
Activation energy for fuel surface decomposition	70,710 kJ/kmol
Heat decomposition of oxidizer	-502 kJ/kg
Density of oxidizer	1950 kg/m^3
Pre-exponential for oxidizer surface decomposition	$4 \cdot 10^6$ kg/m^2·s
Activation energy for oxidizer surface decomposition	96,232 kJ/kmol
Molecular weight of primary flame products	28.00 kg/kmol
Molecular weight of final flame products	20.78 kg/kmol
Pre-exponential for primary flame kinetics	188 s^{-1}
Pre-exponential of oxidizer monopropellant flame kinetics	70,000 s^{-1}
Activation energy for primary flame	62,760 kJ/kmol
Activation energy for oxidizer monopropellant flame	121,336 kJ/kmol
Primary flame reaction order	2.0
Oxidizer monopropellant flame reaction order	1.8
Specific heat of solid and gases	1.255 kJ/kg·K
Viscosity of gases	$5.0 \cdot 10^{-5}$ kg/m·s
Thermal conductivity of gases	$1.255 \cdot 10^{-4}$ kJ/m·k·s
Diffusion parameter	$7.7 \cdot 10^{-5}$ N/K$^{1.75}$·s

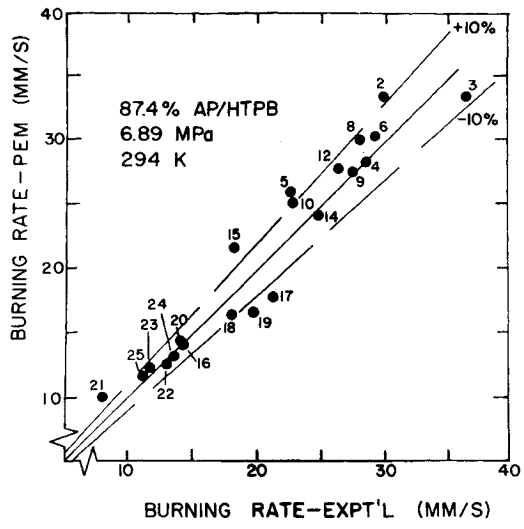

Fig. 2 Burning rate experimental vs theoretical comparison.

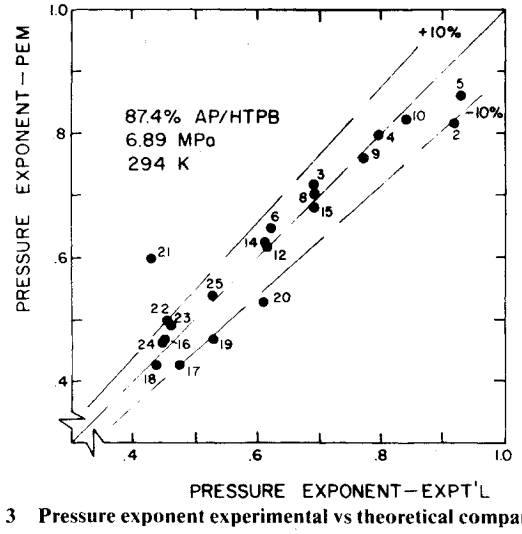

Fig. 3 Pressure exponent experimental vs theoretical comparison.

IV. Computer Propellants

In order to understand fully the effects of oxidizer particle size and size distribution on the combustion properties of polydisperse composite propellants, it is necessary to consider propellants which have a wide range of oxidizer particle sizes and size distributions. Since it is not experimentally feasible to make that many propellants, the propellants used for this part of the study are "computer" propellants whose compositions have been selected to provide the wide range necessary for illustrating the effects of the oxidizer particle size and size distribution. Clearly, the ranges of values selected for the computer propellants are wide enough so that all realistic propellant formulations will be included. Thus, the propellant chemist may understand the effects of wide variations in oxidizer formulations. The value of the solids loading for all of the computer propellants was selected as 87.4%, since the combustion properties at that value showed remarkable agreement with the available experimental burning rate data.

Only two types of "computer" propellants—unimodal and bimodal—are considered. In each case the propellant is a composite having ammonium perchlorate for the oxidizer

with an HTPB fuel binder and no metal additives or catalysts. The necessary propellant constants are those determined by the method described in the previous section.

For the unimodal computer propellants, the weight mean diameter of the individual oxidizer mode has a value ranging from 0.4 to 400 μ. To determine the effect of changing the oxidizer's size distribution, three different mode width parameters are considered: the monodisperse case, $\sigma = 1.0$; and two polydisperse cases, $\sigma = 2.0$ and $\sigma = 3.0$

For the bimodal computer propellants, the coarse oxidizer fraction's weight mean diameter is held constant at 400 μ, while the weight mean diameter for the fine oxidizer fraction is changed in steps from 0.4 to 400 μ. The coarse-to-fine ratio for the bimodal blends is changed in steps, from 40/60 to 70/30, and results were obtained for two particle size distributions ($\sigma = 1.0$ and $\sigma = 2.0$).[9] However, only the polydisperse results are reported.

For all of the computer propellants, the burning rate, pressure exponent, and temperature sensitivity have been computed, and the results are presented to demonstrate the importance of considering both the oxidizer's size and size distribution in propellant formulation studies. The values of burning rate, pressure exponent, and temperature sensitivity are determined for a combustion pressure of 6.89 MPa and an initial solid propellant temperature of 294 K.

V. Results and Discussion

The results of the calculations for the computer propellants can best be understood by first considering the results for the unimodal series of propellants, followed by a consideration of the results for the bimodal series.

Unimodal Propellants

The first series of results are those for the unimodal computer propellants. Figures 4-6 give the calculated values of burning rate, pressure exponent, and temperature sensitivity for the three different values of the mode width parameter σ as a function of the mean diameter $\bar{D}$. For these calculations, the combustion pressure was 6.89 MPa and the initial temperature of the solid propellant was 294 K.

Burning Rate

In Fig. 4, the general S-shaped curve is representative of both experimental[5] and theoretical[2,6,7] burning rate results. The small particles yield high burning rates. As particle size decreases, the burning rate approaches a limiting value determined by the premixed kinetic reaction standoff distance for a kinetically controlled primary flame between the oxidizer and fuel binder. Conversely, the large particles yield low burning rates. As the particle size increases, the burning rate approaches a limiting value determined by the kinetically controlled decomposition of the pure oxidizer. The burning rate for the intermediate diameters is determined by competing processes within each of the three flames above an individual oxidizer particle. The diffusion and kinetic reactions within the primary flame, the kinetic reaction of the monopropellant flame, and the diffusional processes of the final flame all contribute in the overall determination of the burning rate.

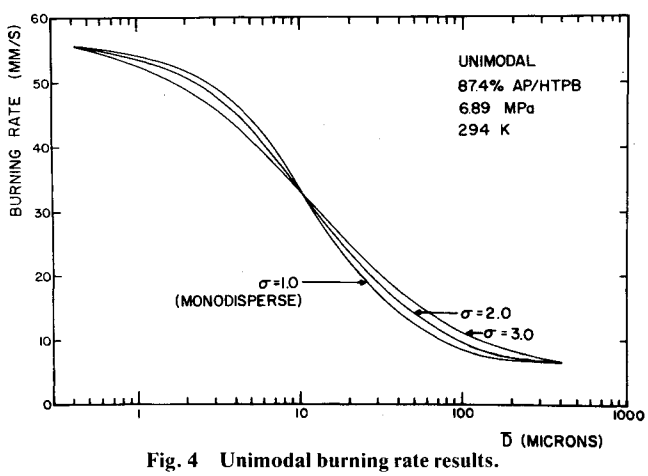

Fig. 4 Unimodal burning rate results.

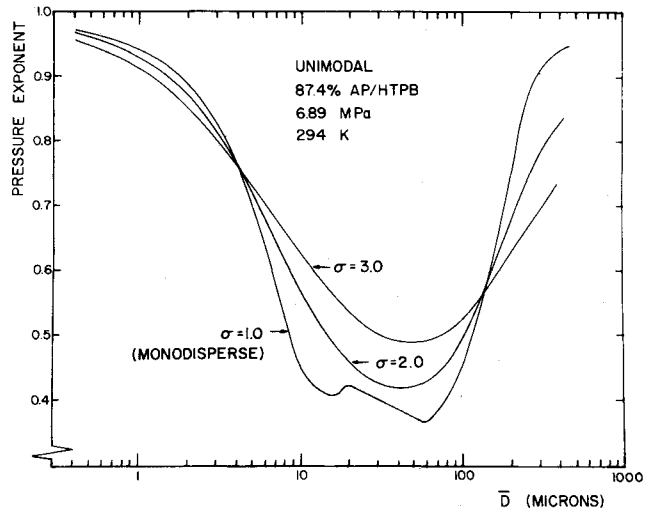

Fig. 5 Unimodal pressure exponent results.

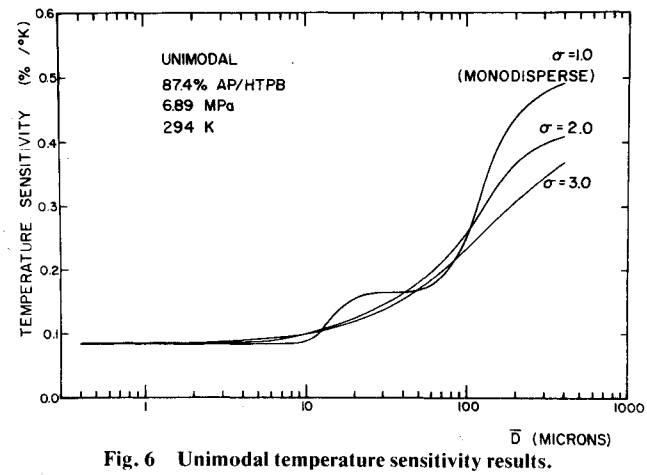

Fig. 6 Unimodal temperature sensitivity results.

In order to explain the variations in the burning rate for the various oxidizer size distributions, it should be emphasized that one of the assumptions in the PEM is that each oxidizer particle burns independently of all the other oxidizer particles within the propellant. Therefore, for any given $\bar{D}$, the burning rate for a polydisperse propellant can be calculated by superpositioning the monodisperse burning rates for particles within the distribution. The effect of widening an oxidizer distribution about some given mean diameter $\bar{D}$ then is dependent on the character of the burning rate results for the oxidizer whose diameters are both larger and smaller than $\bar{D}$ making up a given distribution. If the effect on the total propellant burning rate due to the faster burning smaller particles within the distribution is greater than that of the slower burning larger particles, then an increase in the width of the distribution will result in a corresponding increase in the burning rate. The reverse trend is also true, as can be observed by the results shown in this figure for the unimodal propellants.

Pressure Exponent

The calculated pressure exponent is plotted in Fig. 5 again as a function of the mean diameter $\bar{D}$ and the mode width parameter σ for the unimodal computer propellants. For the

monodisperse ($\sigma = 1.0$) case, the pressure exponent decreases from a near unity value for the submicron size oxidizer particles to a minimum of about 0.4 for intermediate oxidizer diameters between 10 and 100 μ. Above 100 μ, the pressure exponent begins to increase, approaching near unity for the very large oxidizer diameters. To explain the phenomena exhibited by the monodisperse propellants, it is necessary to examine the burning rate behavior predicted by a multiple flame combustion model like the PEM. For a given oxidizer diameter, the effect of pressure on its burning rate indicates that at different pressures, different flames dominate. This competition between the flames surrounding an individual oxidizer crystal greatly affects its burning rate behavior. At low pressures, the burning rate is controlled by the kinetic step in the primary flame, since diffusion distances are small and the oxidizer monopropellant flame and the final diffusion flame are not present. This results in a slope of the rate-pressure curve or a pressure exponent near unity. For increased pressures, the diffusional processes in the primary flame begin to compete with kinetic reactions. With further increases in pressure, the oxidizer monopropellant flame and the final diffusion flame begin to compete with the primary flame in determining the burning rate. The result of these steps is a lowering of the pressure exponent as pressure is increased. Finally, for even higher pressures, the primary flame and the final diffusion flame begin to have a negligible effect on the burning rate, with the oxidizer monopropellant flame becoming the rate-controlling step in the combustion process. This step corresponds to an increased pressure exponent, once again approaching unity.

The same type of flame dependencies and interactions occur in the propellants having different oxidizer sizes; however, the pressures at which these processes occur depend on the oxidizer diameter. For example, it was shown in Ref. 9 that the primary kinetic flame dominates the burning process up to a pressure of 0.5 MPa for a 100 μ particle. This dependency, however, extends up to a pressure of 4 MPa for a 10 μ particle and a pressure of 30 MPa for a fine 1 μ particle. Returning to Fig. 5, the general shape of the pressure exponent vs diameter curve for the monodisperse case is the direct result of the various flame dependencies and interactions decribed previously that are occurring at a pressure of 6.89 MPa for the different size particles.

Having discussed the reasoning behind why the monodisperse pressure exponent vs $\bar{D}$ curve behaves as it does, some mention should be made regarding the effect of considering the size distribution for the oxidizer mode. As was the case with the burning rate for the polydisperse propellants, the calculated pressure exponent for a polydispersion of oxidizer particles will be influenced to some extent by each of the particles within the distribution. For example, for a unimodal propellant with a 50% weight mean diameter of about 40 μ, the pressure exponent calculated for a

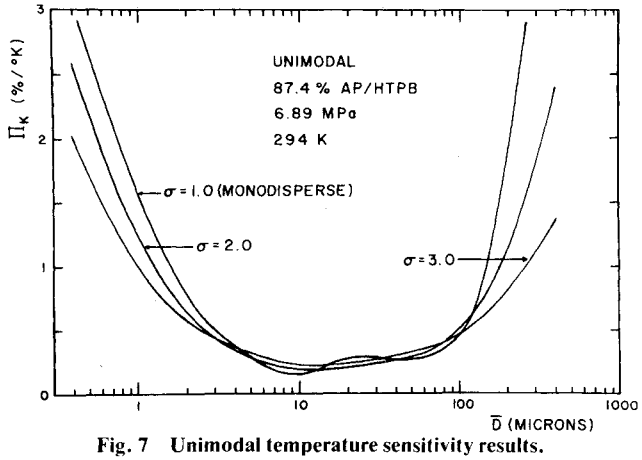

Fig. 7 Unimodal temperature sensitivity results.

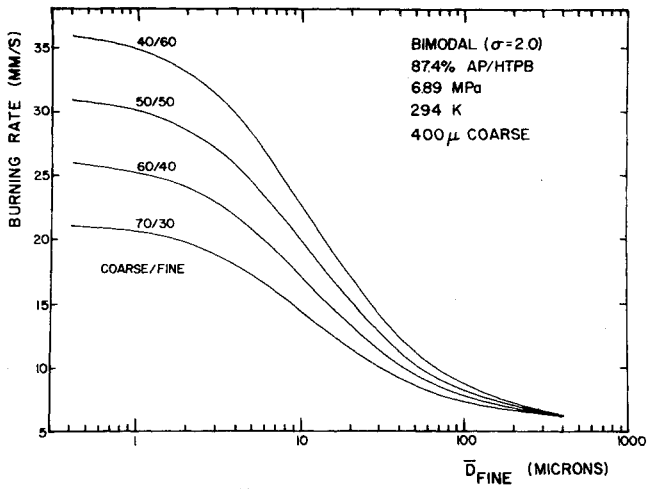

Fig. 8 Bimodal burning rate results.

polydisperse distribution is greater than the pressure exponent obtained for the monodisperse case. To understand this, one need only notice that the monodisperse ($\sigma = 1.0$) curve predicts that particles with diameters both larger and smaller than 40 μ yield an increased pressure exponent. Thus, the overall effect of considering a distribution of oxidizer particles about this mean diameter is to increase the pressure exponent above the value determined for the monodisperse case. Similar reasoning can be applied to any particular $\bar{D}$.

The difference between the pressure exponents calculated for the polydisperse distributions and the monodisperse distribution depend on the shape of the monodisperse curve within the diameter range considered by a distribution. The pressure exponent will be greater for the polydisperse case if the particles in the distribution yielding higher exponents outweigh the effect of the particles in the distribution yielding lower exponents and vice versa.

Temperature Sensitivity

The results of the PEM's calculations for the unimodal temperature sensitivity, σ_p, are presented in Fig. 6. For a mean diameter $\bar{D}$ below 10 μ, the temperature sensitivity was found to be a constant independent of the size distribution considered. However, as the size of the oxidizer increases, the temperature sensitivity increased, becoming, at the same time, a strong function of the mode width parameter. From the pressure exponent results of Fig. 5, it is evident that for a pressure of 6.89 MPa, the burning rate of small diameter oxidizer particles is controlled by the primary flame and the burning rate of the larger particles by the oxidizer monopropellant flame. Therefore, it is apparent from these results that the oxidizer monopropellant flame is more sensitive to changes in initial solid propellant temperature than the primary flame.

The effect of the oxidizer's size distribution on the temperature sensitivity can be explained in a fashion similar to that employed in both the burning rate results and the pressure exponent results.

From these results and the pressure exponent results of Fig. 5, the second temperature sensitivity parameter, π_K, can be obtained as a function of the mean diameter $\bar{D}$ and mode width parameter σ for the unimodal propellants. These results are depicted in Fig. 7.

Bimodal Propellants

Figures 8, 9, and 10 present burning rates, pressure exponents, and temperature sensitivities, respectively, as calculated by the PEM for the bimodal computer propellants. For the bimodal results, the mode width parameter for both the coarse and the fine oxidizer fractions is equal to 2.0, and the coarse fraction mean diameter is held constant at 400 μ.

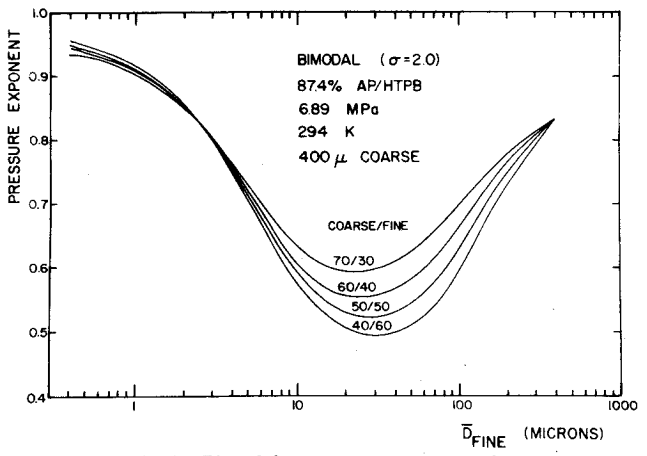

Fig. 9 Bimodal pressure exponent results.

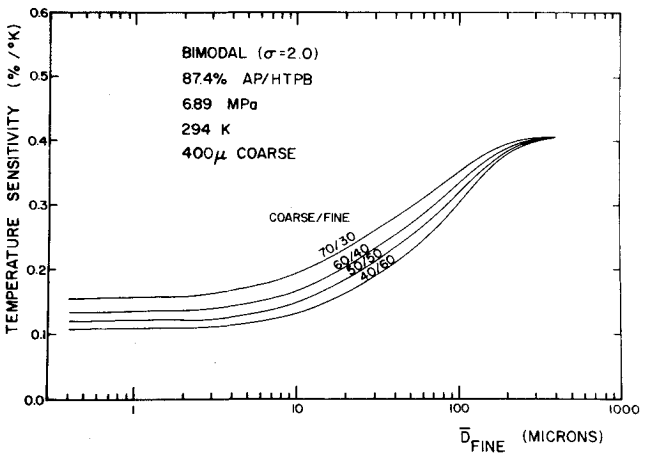

Fig. 10 Bimodal temperature sensitivity results.

In evaluating the resulting calculations for the burning rate, pressure exponent, and temperature sensitivity for the bimodal propellants, the results obtained for the unimodal propellants should be kept in mind. For the unimodal polydisperse cases previously discussed, the overall burning rate, pressure exponent, and temperature sensitivity are shown to be some type of weighted superposition of all the burning rates, pressure exponents, and temperature sensitivities within the distribution, since it is assumed that all oxidizer particles burn independently. In analyzing the bimodal results, it should be evident from the previous discussion that the magnitude of the burning rate, pressure exponent, and temperature sensitivity obtained for a bimodal blend are influenced by the values of these combustion parameters for each mode acting independently as a unimodal propellant. The absolute magnitude of the calculated combustion parameter is also dependent on the coarse-to-fine ratio.

Since the mean diameter of the coarse fraction for each of the bimodal computer propellants is held constant at 400 μ for any coarse-to-fine ratio, the effect on the overall burning rate, pressure exponent, and temperature sensitivity due to the coarse fraction will be a constant factor. Thus, the variation in the calculated combustion parameters is due entirely to the contribution of the fine fraction. With this in mind, the shape of the burning rate, pressure exponent, and temperature sensitivity curves for the designated bimodal computer propellants should show a similar variation with the mean diameter of the fine fraction, $\bar{D}_{\text{fine}}$, as the unimodal propellants did with $\bar{D}$. In Fig. 8 the burning rate obtained for small values of $\bar{D}_{\text{fine}}$ is shown to be highly dependent on the percentage of the fine fraction. This is because the contribution to the overall rate by the small particles comprising the fine fraction is much larger than that of the 400 μ coarse fraction.

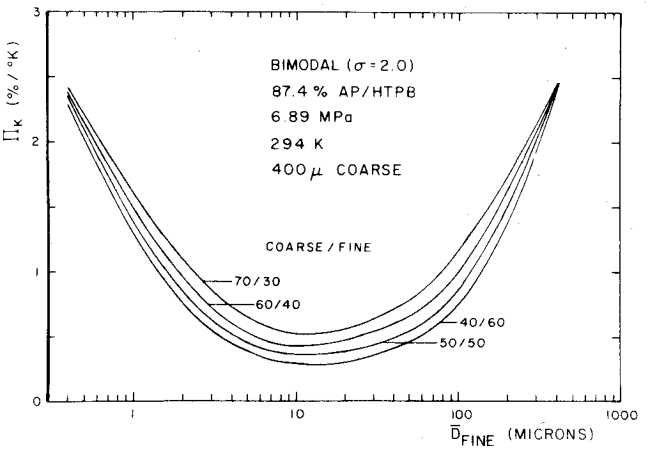

Fig. 11 Bimodal temperature sensitivity results.

Figure 9 indicates that the coarse-to-fine ratio has a significant effect on the bimodal pressure exponent, especially for the intermediate values of $\bar{D}_{\text{fine}}$. The temperature sensitivity results in Fig. 10 conform to a predictable form as the coarse-to-fine ratio is varied. Finally, the temperature sensitivity parameter π_K for bimodal propellants obtained from the two previous figures is presented in Fig. 11.

VI. Conclusions

It may be concluded that the Petite Ensemble Model has the ability to predict the burning rates and pressure exponents for a series of AP/HTPB proprellants within 10% of the experimental values. It is concluded that this exceptional predictive capability is the result of the model's capability of describing both size and size distribution of the oxidizer particles within the burning rate calculations.

By using the PEM, the burning rate, pressure exponent, and temperature sensitivity were calculated for a series of computer propellants, unimodal and bimodal, and the results were reported. For the unimodal propellants, the oxidizer size had a predictable effect upon the calculated combustion parameters. But more important, it was shown that the oxidizer size distribution has a substantial effect upon the burning rate, pressure exponent, and temperature sensitivity. In each case, the particular effect was related to a specific flame, and the trends were shown to be dependent on the flame structure in a manner that agreed with the available experimental data.

For the bimodal distributions, the results were consistent with those that could be inferred from the unimodal results. With these propellants, the burning rate, pressure exponent, and temperature sensitivity were shown to be strong functions of the coarse-to-fine ratio and the mean diameter of the fine fraction.

Finally, it may be concluded that the PEM is unique in its ability to predict the effects of the oxidizer size distribution on the combustion characteristics of the composite solid propellant.

VII. Acknowledgment

Research sponsored by the Air Force Office of Scientific Research, Air Force Systems Command, USAF, under Grant No. AFOSR-77-3381. The United States Government is authorized to reproduce and distribute reprints for governmental purposes notwithstanding any copyright notation hereon.

VIII. References

[1]Glick, R.L., "On Statistical Analysis of Composite Solid Propellant Combustion," *AIAA Journal*, Vol. 12, March 1974, pp. 384-385.

[2]Beckstead, M.W., Derr, R.L., and Price, C.F., "A Model of Composite Solid Propellant Combustion Based on Multiple Flames," *AIAA Journal*, Vol. 8, No. 4, Dec. 1970, pp. 2200-2207.

[3]Glick, R.L. and Condon, J.A., "Statistical Analysis of Polydisperse, Heterogeneous Propellant Combustion: Steady State," *Thirteenth JANNAF Combustion Meeting*, CPIA Publication 281, Vol. II, Dec. 1976, pp. 313-345.

[4]Condon, J.A. and Osborn, J.R., "The Effect of Oxidizer Particle Size Distribution on the Steady and Nonsteady Combustion of Composite Propellants," AFRPL-TR-78-17, June 1978.

[5]Miller, R.R., Donohue, M.T., and Martin, J.R., "Control of Solids Distribution: I - Ballistics of Non-aluminized HTPB Propellants," *Thirteenth JANNAF Combustion Meeting*, CPIA Publication 281, Vol. II, Dec. 1976, pp. 1-18.

[6]Summerfield, M., Sutherland, G.S., Webb, M.J., Taback, H.J., and Hall, K.P., "Burning Mechanism of Ammonium Perchlorate Propellants," *ARS Progress in Astronautics and Rocketry Vol. I: Solid Propellant Rocket Research*, Academic Press, New York, 1960, pp. 141-182.

[7]Hermance, C.E., "A Model of Composite Propellant Combustion Including Surface Heterogeneity and Heat Generation," *AIAA Journal*, Vol. 4, Sept. 1966, pp. 1629-1637.

[8]Renie, J.P. and Osborn, J.R., "The Implicit Flame Interaction Model," *Fifteenth JANNAF Combustion Meeting* (in press).

[9]Renie, J.P., Condon, J.A., and Osborn, J.R., "Oxidizer Distribution Effects," *Fourteenth JANNAF Combustion Meeting*, CPIA Publication 292, Vol. I, Dec. 1977, pp. 325-339.

From the AIAA Progress in Astronautics and Aeronautics Series . . .

INTERIOR BALLISTICS OF GUNS—v. 66

Edited by Herman Krier, University of Illinois at Urbana-Champaign, and Martin Summerfield, New York University

In planning this new volume of the Series, the volume editors were motivated by the realization that, although the science of interior ballistics has advanced markedly in the past three decades and especially in the decade since 1970, there exists no systematic textbook or monograph today that covers the new and important developments. This volume, composed entirely of chapters written specially to fill this gap by authors invited for their particular expert knowledge, was therefore planned in part as a textbook, with systematic coverage of the field as seen by the editors.

Three new factors have entered ballistic theory during the past decade, each it so happened from a stream of science not directly related to interior ballistics. First and foremost was the detailed treatment of the combustion phase of the ballistic cycle, including the details of localized ignition and flame spreading, a method of analysis drawn largely from rocket propulsion theory. The second was the formulation of the dynamical fluid-flow equations in two-phase flow form with appropriate relations for the interactions of the two phases. The third is what made it possible to incorporate the first two factors, namely, the use of advanced computers to solve the partial differential equations describing the nonsteady two-phase burning fluid-flow system.

The book is not restricted to theoretical developments alone. Attention is given to many of today's practical questions, particularly as those questions are illuminated by the newly developed theoretical methods. It will be seen in several of the articles that many pathologies of interior ballistics, hitherto called practical problems and relegated to empirical description and treatment, are yielding to theoretical analysis by means of the newer methods of interior ballistics. In this way, the book constitutes a combined treatment of theroy and practice. It is the belief of the editors that applied scientists in many fields will find material of interest in this volume.

385 pp., 6 × 9, illus., $25.00 Mem., $40.00 List

TO ORDER WRITE: Publications Dept., AIAA, 1290 Avenue of the Americas, New York, N. Y. 10019